Alterations of the trabecular pattern of the jaws in patients with osteoporosis

Stuart C. White, DDS, PhD,[a] and David J. Rudolph, DDS, MS, PhD,[b] Los Angeles, Calif
UCLA SCHOOL OF DENTISTRY

Objective. The purpose of this study was to determine whether the morphologic features of the trabecular bones of the maxilla and mandible differ between patients with osteoporosis and normal controls.
Study design. Periapical radiographs, obtained from dentists of 11 patients with osteoporosis and 12 control subjects, were digitized at 600 dpi. A custom computer program measured morphologic features of the trabecular architecture. The mean values for each feature were determined for the osteoporotic and control groups and compared by anatomic site.
Results. Twenty-four morphologic features of the trabeculae and marrow regions were examined in each anatomical site. A principal components analysis summarized these predictors to four. The Hotelling T^2 test found that patients with osteoporosis had significantly altered morphologic pattern in the anterior maxilla ($P = .019$) and the posterior mandible ($P = .013$) in comparison with the controls. A classification tree analysis separated all subjects into 2 groups with 92% accuracy.
Conclusions. The data support the hypothesis that patients with osteoporosis have an altered trabecular pattern in the jaws in comparison with normal subjects.
(Oral Surg Oral Med Oral Pathol Oral Radiol Endod 1999;88:628-35)

Osteoporosis is a metabolic bone disease characterized by low bone mass and microarchitectural deterioration of bone tissue leading to enhanced bone fragility and an increased risk of fracture.[1] It is one of the most common metabolic bone disorders in the elderly, affecting approximately 30% of postmenopausal women.[2] Fractures involve primarily the spine, hip, wrist, and proximal humerus. Those involving the hip are particularly devastating, with 20% of patients dying from their injuries. Encouragingly, there are now multiple means of treating this condition.

The World Health Organization defines *osteoporosis* as a bone mineral density (BMD) greater than 2.5 standard deviations below the young adult mean BMD.[2] Bone mass is usually measured by determining the BMD of trabecular or cortical bone through use of cross-sectional imaging based on quantitative computed tomography[3,4] or of the whole bone through use of dual energy x-ray absorptiometry (DEXA).[5] Because osteoporosis results in a greater relative loss of trabecular than of cortical bone, quantitative computed tomography provides the better method of examination.[6,7] DEXA scans, which measure the entire bone, are usually used because they have a lower radiation dose and are characterized by better precision and greater ease of use.[2] However, the costs associated with these advanced imaging techniques, as well as the distribution of the equipment, limits their usefulness for screening examinations.

There are 2 primary mechanisms of loss of trabecular bone: rapid loss associated with osteoclastic destruction, presenting perforations of the trabeculae, and slow bone loss, presenting as decreased osteoblastic depositing, which results in thinning of the bone.[8-10] When bone becomes sufficiently demineralized, skeletal fractures occur. The age at which this critical fracture threshold is reached depends on the maximal bone mass achieved in early adulthood and the rate of loss with increasing age. Other risk factors for osteoporosis include cigarette smoking, alcohol abuse, physical inactivity, low dietary calcium, and the presence of systemic disease, including hyperparathyroidism and rheumatoid arthritis.[11,12] There is developing evidence that bone structure, in addition to mass, is important in determining bone strength.[9,13-16] Bone trabecular pattern can be characterized by a number of measures, including area of the bony plates, circumference of the trabeculae, number of bony and marrow regions, thickness of trabeculae, trabecular spacing,[9,17-22] and osseous fractal dimension.[22-26] A means of analyzing architectural features of the trabecular pattern from conventional radiographs has been described.[27,28] Morphologic features of the trabecular pattern of the distal radius were measured and found to correlate with the bone mineral density of the lumbar spine.[29]

With their high spatial resolution (in comparison with that of computed tomographs), dental radiographs of the basal and alveolar bone of osteoporotic men and women may reveal changes in morphologic features of bone trabeculation compared with unaffected individuals. If

Portions of the data in this manuscript were presented at the 49th Annual Session of the American Academy of Oral and Maxillofacial Radiology held in Santa Fe, NM, 1998.
[a]Professor, Section of Oral Radiology.
[b]Assistant Professor, Section of Orthodontics.
Received for publication Feb 8, 1999; returned for revision Apr 3, 1999; accepted for publication May 28, 1999.

1079-2104/99/$8.00 + 0 **7/16/100548**

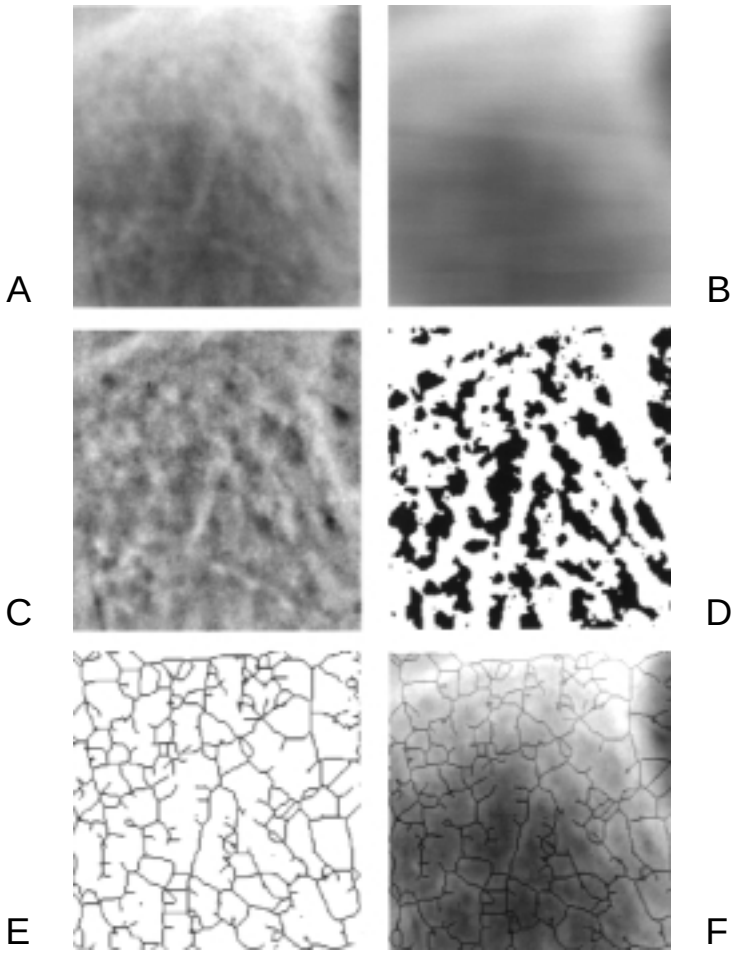

Fig 1. **A,** Region of interest of trabecular bone from digitized radiograph of anterior maxilla. **B,** Result of blurring of region seen in Fig 1, *A*. **C,** Result of subtracting Fig 1, *B* from Fig 1, *A* and adding 128. **D,** Binary version of Fig 1, *C*. **E,** Trabecular pattern (white region of Fig 1, *D*) is skeletonized. **F,** Addition of images A and E to visually demonstrate that skeletonized image corresponds to original trabeculae. Note that Fig 1, *C* shows trabecular detail even in dark and light regions of image.

appropriate bone features that identify patients showing early signs of osteoporosis can be found on dental radiographs, then dentists will be able to provide a valuable screening service for their patients by referring appropriate patients to their physicians for follow-up.

The purpose of this study was to test our hypothesis that the morphologic features of the trabecular bone of the maxilla and mandible differ between patients with osteoporosis and normal control subjects.

METHODS AND MATERIAL

Custom trabecular bone morphology program

Using NIH Image software, we wrote a custom computer program that measures morphologic features of the trabecular architecture in digitized radiographs.[30] This program uses methods described both in studies of the trabeculae of the distal radius involving conventional radiographs[27-28] and in studies of the trabecular pattern of bone in histologic slides.[18-20]

To begin, the user identifies a region of interest in the radiograph (Fig 1, *A*). The program is designed to remove large-scale variations in brightness on the image; such variations have various causes—eg, differences in thickness of the object or the presence of partially overlapping soft tissue. To accomplish this task, the region of interest is blurred through use of a Gaussian filter (sigma = 35 pixels, kernel size = 33 × 33; Fig 1, *B*). This step removes all fine-scale and medium-scale structure and retains only large variations in density (low-pass filtering). The resulting heavily blurred image is then subtracted from the original, and 128 is added to the result at each pixel location (Fig 1, *C*). This generates an image with a mean value of 128, regardless of the initial intensity of the

Table I. Summary statistics: maxilla

	Anterior maxilla					*Posterior maxilla*				
	Osteoporosis		*Control*			*Osteoporosis*		*Control*		
Morphologic feature	*n = 10*	*SD*	*n = 12*	*SD*	*P value*	*n = 5*	*SD*	*n = 7*	*SD*	*P value*
Trabeculae										
Trabecular area/total area	0.49	0.04	0.54	0.04	.006*	0.48	0.03	0.52	0.03	.036*
Periphery/total area	0.21	0.03	0.25	0.03	.004*	0.23	0.03	0.27	0.02	.061
Periphery/trabecular area	0.42	0.05	0.47	0.04	.050	0.49	0.05	0.52	0.04	.225
Length/trabecular area	0.15	0.01	0.15	0.01	.698	0.15	0.01	0.15	0.01	.988
Length/total area	0.07	0.01	0.08	0.01	.028*	0.07	0.01	0.08	0.01	.243
Terminal points/sq cm	632	169	894	195	.003*	840	182	1154	152	.014*
Terminal points/length	0.16	0.03	0.20	0.03	.006*	0.21	0.04	0.27	0.03	.026*
Terminal points/periphery	0.05	0.01	0.06	0.01	.007*	0.06	0.01	0.08	0.00	.004*
Terminal points/trabecular area	0.02	0.01	0.03	0.01	.011*	0.03	0.01	0.04	0.00	.030*
Branch points/sq cm	265	50	309	52	.059	236	54	239	55	.935
Branch points/length	0.07	0.01	0.07	0.01	.280	0.06	0.01	0.05	0.01	.300
Branch points/periphery	0.02	0.00	0.02	0.00	.462	0.02	0.00	0.02	0.00	.278
Branch points/trabecular area	0.01	0.00	0.01	0.00	.390	0.01	0.00	0.01	0.00	.467
Branch points/terminal points	0.44	0.09	0.36	0.08	.036*	0.29	0.07	0.21	0.06	.078
Marrow										
Marrow area/total area	0.51	0.04	0.46	0.04	.006*	0.52	0.03	0.48	0.03	.036*
Length/marrow area	0.19	0.03	0.24	0.02	.003*	0.22	0.03	0.26	0.02	.033*
Length/total area	0.10	0.01	0.11	0.01	.065	0.11	0.01	0.12	0.01	.147
Terminal points/sq cm	484	139	728	186	.002*	589	166	812	116	.037*
Terminal points/length	0.09	0.02	0.12	0.03	.004*	0.09	0.02	0.12	0.02	.052
Terminal points/marrow area	0.02	0.01	0.03	0.01	.002*	0.02	0.01	0.03	0.01	.029*
Branch points/sq cm	462	98	529	70	.089	576	70	633	98	.267
Branch points/length	0.08	0.01	0.09	0.01	.156	0.09	0.00	0.09	0.01	.620
Branch points/marrow area	0.02	0.00	0.02	0.00	.007*	0.02	0.00	0.02	0.00	.058
Branch points/terminal points	0.99	0.17	0.77	0.23	.022*	1.03	0.23	0.80	0.18	.101

*$P \leq .05$.

image. The idea is that individual variations in this image (brightness levels) then reflect particular types of features, in this case trabeculae and marrow spaces.

The image is then made binary, thresholding on a brightness value of 128 and thus segmenting the image into components that visually (radiographically) approximate the trabeculae and marrow (Fig 1, *D*). The resultant image is eroded and dilated once to reduce noise. The image of the trabeculae is then inverted to make the trabeculae and then skeletonized—that is, eroded until only the central line of pixels remains (Fig 1, *E*). Superimposition of the skeletonized trabecular image on the original image of the bone demonstrates that the skeletal structure studied corresponds to the trabeculae of the original image (Fig 1, *F*).

We analyzed the binary and skeletonized images to determine the morphologic features of the selected area of the radiograph. Trabecular area represents the total number of black pixels in the binary image divided by the total number of pixels in the region of interest. The periphery represents the total number of pixels on the outer border of the trabeculae in binary images, presented as a proportion of the total area of the trabeculae or of the total region of interest. In the skeletonized image, we computed the total length of the skeletonized trabeculae (total number of black pixels), the number of terminal points (free ends, ie, black pixels each having only 1 adjacent black pixel), and the number of branch points (crossing points, ie, black pixels each having 3 or more adjacent black pixels). These parameters are expressed as a proportion of trabecular length, area, and perimeter. The marrow area was similarly examined by inverting the image (making the marrow area black) and then skeletonizing the resultant image to its core marrow structure.

Patients

Osteoporotic patients were identified at the UCLA Osteoporosis Center. Each of these patients had BMDs of the spine and hip measured through use of a DEXA scan. Those consenting individuals with BMD values greater than 2.5 SDs below the mean for young women for at least 1 site and having no sites less than 1 SD below normal at other sites were defined as having osteoporosis for the purposes of this study. From this patient pool we obtained intraoral radiographs for 11 patients (mean age, 63.1 years). The exposure factors were unknown. Radiographs were also collected from 12 control patients seek-

Table II. Summary statistics: mandible

	Anterior mandible					*Posterior mandible*				
	Osteoporosis		*Control*			*Osteoporosis*		*Control*		
Morphologic feature	*n = 9*	*SD*	*n = 11*	*SD*	*P value*	*n = 7*	*SD*	*n = 10*	*SD*	*P value*
Trabeculae										
Trabecular area/total area	0.51	0.07	0.56	0.03	.075	0.48	0.06	0.54	0.03	.048*
Periphery/total area	0.23	0.06	0.28	0.04	.051	0.23	0.03	0.29	0.03	.005*
Periphery/trabecular area	0.46	0.06	0.51	0.06	.080	0.48	0.03	0.53	0.04	.007*
Length/trabecular area	0.15	0.01	0.15	0.01	.169	0.14	0.01	0.15	0.01	.127
Length/total area	0.07	0.02	0.09	0.01	.078	0.07	0.01	0.08	0.00	.056
Terminal points/sq cm	831	274	1080	260	.054	815	208	1150	182	.005*
Terminal points/length	0.20	0.03	0.23	0.04	.114	0.21	0.03	0.26	0.04	.010*
Terminal points/periphery	0.06	0.01	0.07	0.01	.166	0.06	0.01	0.07	0.01	.018*
Terminal points/trabecular area	0.03	0.01	0.03	0.01	.089	0.03	0.01	0.04	0.00	.006*
Branch points/sq cm	276	76	324	23	.102	242	72	276	50	.309
Branch points/length	0.07	0.01	0.07	0.00	.337	0.06	0.01	0.06	0.01	.921
Branch points/periphery	0.02	0.00	0.02	0.00	.900	0.02	0.00	0.02	0.00	.668
Branch points/trabecular area	0.01	0.00	0.01	0.00	.184	0.01	0.00	0.01	0.00	.615
Branch points/terminal points	0.34	0.07	0.32	0.10	.588	0.30	0.05	0.25	0.08	.124
Marrow										
Marrow area/total area	0.49	0.07	0.44	0.03	.075	0.52	0.06	0.46	0.03	.048*
Length/marrow area	0.22	0.04	0.26	0.03	.059	0.22	0.04	0.26	0.02	.031*
Length/total area	0.11	0.01	0.11	0.01	.155	0.11	0.01	0.12	0.01	.125
Terminal points/sq cm	635	258	862	200	.047*	572	190	851	127	.007*
Terminal points/length	0.10	0.04	0.14	0.03	.047*	0.09	0.03	0.13	0.02	.010*
Terminal points/marrow area	0.02	0.01	0.04	0.01	.046*	0.02	0.01	0.03	0.01	.010*
Branch points/sq cm	541	49	566	67	.347	595	86	604	62	.828
Branch points/length	0.09	0.00	0.09	0.01	.798	0.09	0.01	0.09	0.01	.219
Branch points/marrow area	0.02	0.00	0.02	0.00	.078	0.02	0.00	0.02	0.00	.208
Branch points/terminal points	0.997	0.42	0.69	0.18	.072	1.12	0.29	0.73	0.15	.011*

*$P \leq .05$.

ing general dental care and having no history of osteoporosis (mean age, 39.3 years). These radiographs were exposed at 70 kVp, 15 mA, and variable exposure time through use of Ektaspeed Plus film (Kodak). Informed consent was obtained from all subjects in the study.

Radiographs

All periapical radiographs from osteoporotic and control patients were digitized at 600 dpi on an Afga Arcus II scanner. Because of the possibility of alterations in the trabecular pattern as a result of odontogenic factors, we selected sites as remote from the dentition as possible. Images of basal bone in the anterior regions and alveolar bone in the posterior regions were selected from the following sites: (1) anterior maxilla superior to the apices of the incisors; (2) anterior mandible inferior to the incisors; (3) posterior maxilla posterior to the last molar and inferior to the maxillary sinus; and (4) posterior mandible posterior to the last molar and superior to the inferior alveolar nerve canal. In each instance an effort was made to select as large a region as possible, the apices of teeth being avoided. The sites were individually analyzed through use of the program described.

Statistical analysis

The mean values for each of the parameters listed in Tables I and II were determined for the osteoporotic and control groups by anatomical site. Because of the large number of predictor variables and comparisons relative to the sample sizes, we used a principal components analysis to summarize the number of predictors to four in each anatomical region. A Hotelling T^2 test was then used on these 4 variables to determine whether the overall mean differences in outcome at each of the 4 sites were beyond chance. The means were compared by means of the Student *t* test through use of a 2-tailed distribution and 2 samples of unequal variance. Significance was defined as $P \leq .05$.

Because this was an exploratory study, we also performed a multivariate analysis using classification trees. The Cox-Snell R^2 was used to estimate the proportion of disease variation explained by the predictors.

RESULTS

Table I presents summary statistics for the morphologic features found in the trabeculae of the maxilla; Table II shows the findings in the mandible. Compared with control individuals, patients with osteoporosis demon-

Table III. Multiple comparisons correction

Location	No. of observations/ group	Variance accounted for (%)	Hotelling F-statistic	P value
Anterior maxilla	22	97.7	3.93	.019
Posterior maxilla	12	97.7	3.39	.221
Anterior mandible	20	98.6	1.15	.369
Posterior mandible	17	98.4	5.06	.013

strate a reduction in the area of trabeculae and length of the periphery of the trabeculae bone in the region of interest. There is also a reduction in the complexity of the trabecular pattern of osteoporotic patients in comparison with control individuals, as shown by a reduction in the number of terminal points, considered either as an absolute count per area or as a function of skeletal length, length of periphery of trabeculae, or trabecular area. The marrow pattern is similar in that there is a corresponding increase in marrow area but also a general reduction in marrow complexity, as shown by a reduction in the number of terminal points. This pattern is consistent throughout the jaws. The number of branch points, either in absolute terms or as a function of trabecular periphery, length, or area, does not differ between patients with osteoporosis and control individuals. However, with regard to the *P* values in Tables I and II, because the Hotelling T^2 is only significant in the anterior maxilla and the posterior mandible, the nominally significant *P* values in the posterior maxilla and anterior mandible are likely to be artifacts of repeated significance testing and the low sample size. Tables I and II should thus be regarded as more descriptive in nature.

Table III shows the results of the principal components analysis. For each anatomical location, 4 variables were developed that accounted for 98% of the variance. The Hotelling T^2 test showed that statistically significant differences between osteoporotic patients and controls individuals are found in the anterior maxilla and the posterior mandible.

Although this was an exploratory study, we performed a multivariate analysis using classification trees. The classification tree is shown in Fig 2. The subjects are first divided into 2 groups according to the ratio of the number of terminal points to the number of periphery pixels in the anterior maxilla (greater or less than 0.0605). One group consists of only 8 control individuals; the second group is mixed. The latter group is then divided according to the number of periphery pixels per trabecular area pixel in the posterior mandible (greater or less than 0.5178) into 2 groups, one consisting of only 3 control individuals and the other consisting of all the patients with osteoporosis and 2 control individuals. This simple algorithm thus correctly categorized 23 (92%) of the 25 study subjects. The Cox-Snell R^2 statistic was 0.81; that is, approximately 81% of the variation of disease was accounted for by the tree. However, this estimate may be too high because of the small sample size.

DISCUSSION

The data presented in this report support the hypothesis that patients with osteoporosis have an altered trabecular pattern in the jaws compared with control individuals. It is known that osteoporosis results in reduction of bone mineral density of the mandible.[24,31-41] Other studies have also demonstrated alterations of the trabecular pattern in demineralized human maxilla[25,42]; our study extends these findings in the jaws to include structural alterations of the trabecular pattern in patients with osteoporosis. Geraets et al[27,29] have shown that these trabecular changes in the distal radius correlate with bone mineral density in the lumbar spine; the changes in trabecular architecture are consistent with the changes in the jaws described in our study. This suggests that cancellous bone in the jaws may respond similarly to other cancellous bone in patients with osteoporosis.

Comparable changes in the architecture of trabecular bone in patients with osteoporosis and in normal aging have been reported in the iliac crest,[17,18,20,43-45] femoral neck,[46] vertebrae,[21,47-50] and distal radius.[27,29] Indeed, Croucher et al[18] have argued that because the architectural changes in patients with osteoporosis correlate with the cancellous bone area and the pattern of changes is the same as that seen in normal aging, primary osteoporosis is the result of greater biologic aging rather than a specific disease process. Regardless of the cause (increasing age or disease), patients with osteoporosis show a decrease in the area of cancellous bone and in the number and thickness of trabecular plates. Typically there is also a decrease in architectural complexity, as demonstrated in this study by a decrease in the number of terminal points per unit area and as a function of trabecular area, periphery, and skeletal length. It is noteworthy that in this study the number of trabecular terminal points per square centimeter is reduced in patients with osteoporosis compared with control individuals, whereas the number of branch points per square centimeter is not. It is probable that the number of terminal points better reflects the fine structure of the trabeculae that is most readily resorbed with osteoporosis while the measures of branch points reflect the core trabecular structure, less readily altered by osteoporosis. Similarly, the length of the skeletonized trabeculae, another measure of the core trabecular structure, also does not distinguish between these 2 groups.

The measures of the trabecular architecture in the jaws reported here are essentially independent of the orientation of the x-ray beam with respect to the

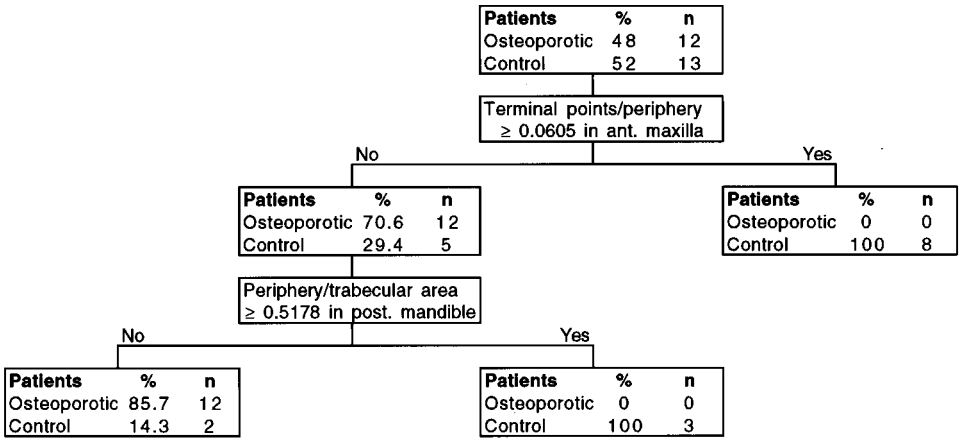

Fig 2. Classification tree shows separation of patients with osteoporosis from control individuals. First step identifies individuals with more than 0.0605 terminal points per periphery pixel in anterior maxilla; second step separates individuals with more than 0.5178 periphery pixels per trabecular area pixel in posterior mandible. This algorithm results in correct classification of 23/25 subjects.

patient, and many are also independent of the optical density of the original radiograph over the diagnostic range.[51] There is still an opportunity to further optimize the characterization of the trabecular and marrow components of the bone. In particular, the specific sequence of erosion and dilation used to smooth the image, as well as the brightness threshold value selected to make the image binary, has a substantive influence on the image appearance. These and other parameters need to be examined in greater detail.

It is of particular significance that the data in this study were collected from conventional dental radiographs made by community dentists in the course of routine dental care. Such images typically have a great range in density and contrast because of variations in exposure conditions, patient, and film procession conditions. Because of this we are specifically interested in assays that do not directly consider the optical density of bone on radiographs. This situation is not aided by the use of direct digital imaging, as the same variables pertaining to exposure and the patient apply. Rather, the key is to develop an assay that examines intrinsic morphologic features of the trabecular bone that are essentially independent of exposure and processing variables. Such an assay is appropriate for use in general dental offices. No special means were used to standardize exposure or processing conditions, and no stepwedge or other such device is needed for image standardization or calibration. As dental offices move to digital imaging, either through direct capture or indirectly by digitization of radiographs, it is easy to imagine development of a module that will analyze the trabecular pattern of bone of all images. Such a process is well suited as a screening examination, as it could be performed on a large number of patients through use of radiographs already collected for diagnostic purposes.

The propensity for the anterior maxilla to be the most sensitive site for distinguishing osteoporotic patients from controls is most likely a consequence of the relatively large amount of trabecular bone and the relatively low cortical bone thickness at this site.[52] The ratio of trabecular to cortical bone is higher in the maxilla because of the relatively dense buccal and lingual cortical plates of the mandible. The skeleton as a whole is composed of approximately 80% cortical bone and 20% trabecular bone.[53] The appendicular skeleton is largely cortical bone, whereas trabecular bone predominates in the vertebral bodies of the spine. Because of its high surface area–to–volume ratio, the trabecular bone is believed to have an 8-fold higher turnover rate than cortical bone and to be highly responsive to metabolic stimuli. The clinical and epidemiologic finding that osteoporotic fractures occur first in the vertebral bodies and distal radius, sites that are predominately trabecular bone, substantiate physiologic studies of early loss of trabecular bone.[53] This observation is of particular interest to our project because the maxillary and mandibular alveolar bones are rich in trabecular bone, particularly in the anterior regions. It must be recognized, however, that it is not clear what structures give rise to the trabecular pattern seen on dental radiographs. Bender and Seltzer[54] showed that removal of cancellous bone from the posterior region of cadaver mandibles did not alter the radiographic appearance of the trabeculae. It was only when the endosteal surface of the cortical bone was removed that the radiographic image was

altered. This finding may not hold true in the maxilla, however, as there the cortical bone is thinner and the cancellous bone more dense. Accordingly, the actual source of the radiographic trabecular pattern studied in this report, cancellous or endosteal cortical bone, may vary with anatomical region.

This exploratory study has limitations that restrict the scope of its conclusions. First, the sample size was small. More patients need to be investigated to gain a better understanding of the intrapatient and interpatient variability of the parameters measured. Furthermore, all patients in this study were women; no data from men has been collected. In addition, the medical histories of the patients with osteoporosis, other than their BMD findings, are unknown. For instance, it is not known how many years have elapsed since menopause or whether the patients are taking hormone replacement therapy. Social factors such as extent of smoking and alcohol consumption, amount of exercise, and nutritional supplements are also not known. Thus, although our results suggest that patients with osteoporosis have differences in the morphologic structure of their trabecular bone, more work is necessary to substantiate these findings in well-defined patient populations in which the conditions mentioned are controlled for.

Our goal is to identify a sensitive and specific screening tool that can be used prospectively to identify individuals with osteoporosis to initiate therapy and forestall or prevent osteoporosis and its disabling consequences. Individual rather than population-based risk assessment is designed to assist a clinician in evaluating a patient's disease risk. Individual risk assessment is clearly indicated when identification of risk and implementation of appropriate preventive measures can effectively help a patient avoid future health problems. Currently there is considerable overlap among the range of values of the morphologic features between controls and patients with osteoporosis. Eventually we wish to identify combinations of morphologic features so that individual risk estimates for osteoporosis can be assigned. Such information would allow dentists to effectively screen a large fraction of the population for osteoporosis and to selectively refer appropriate patients to their physicians for appropriate care. This mechanism of referral may well identify a patient before his or her first fracture. It will also expand the range of services dentists can provide their patients.

APPENDIX

Erosion. Removal of pixels from the edges of objects in a binary image, where contiguous black areas in the image are considered objects and background is assumed to be white. A pixel is removed (set to white) if 4 or more of its 8 neighbors are white. Erosion separates objects that are touching and removes isolated pixels.[30]

Dilation. Addition of pixels to the edges of objects in binary images. A pixel is added (set to black) if 4 or more of its 8 neighbors are black. Dilation connects discontinuous objects and fills in holes.[30]

Gaussian filtration. Blurring accomplished through use of a 33×33 pixel kernel. The weights in each pixel were chosen to simulate a Gaussian distribution. We elected to use a kernel with an SD (sigma) of 35 pixels—ie, the radius containing 68% of the integrated magnitude of the coefficients.[55]

Skeletonization. Repeated removal of pixels from the edges of objects in a binary image until they are reduced to single pixel–wide skeletons.[30]

We gratefully acknowledge the assistance of Dr Aurelia Nattiv and Ms Kathleen Lozano of the UCLA Osteoporosis Center in securing osteoporosis patients for this study. We also thank Ms Cynthia Cheung, Ms Allison Chen, and Mr Ray Kim for their assistance with obtaining and digitizing the radiographs, Dr Sharon Hunt Gerardo for her review of this manuscript, and Ms Margaret Farrell-Ross and Dr Jeffery Gornbein for their help with the statistical analysis.

REFERENCES

1. Lindsay R, Christiansen C, Einhorn TA, McKay Hart D, Ljunghall S, Mutalen CA, et al. Who are candidates for prevention and treatment for osteoporosis? Osteoporos Int 1997;7:1-6.
2. Lenchik L, Sartoris DJ. Current concepts in osteoporosis. AJR Am J Roentgenol 1997;168:905-11.
3. Wahner HW, Riggs BL. Methods and application of bone densitometry in clinical diagnosis. Crit Rev Clin Lab Sci 1986;24:217-33.
4. Rosenthal DI, Ganott MA, Wyshak G, Slovik DM, Doppelt SH, Neer RM. Quantitative computed tomography for spinal density measurement: factors affecting precision. Invest Radiol 1985;20:306-10.
5. Pouilles JM, Tremollieres F, Todorovsky N, Ribot C. Precision and sensitivity of dual-energy x-ray absorptiometry in spinal osteoporosis. J Bone Miner Res 1991;6:997-1002.
6. Genant HK, Block JE, Steiger P, Glueer CC, Smith R. Quantitative computed tomography in assessment of osteoporosis. Semin Nucl Med 1987;17:316-33.
7. Cummings SR, Kelsey JL, Nevitt MC, O'Dowd KJ. Epidemiology of osteoporosis and osteoporotic fractures. Epidemiol Rev 1985;7:178-208.
8. Parfitt AM. Age-related structural changes in trabecular and cortical bone: cellular mechanisms and biomechanical consequences. Calcif Tissue Int 1984:36 (suppl 1):S123-S128.
9. Parfitt AM. Trabecular bone architecture in the pathogenesis and prevention of fracture. Am J Med 1987;82:68-72.
10. Eriksen EF, Hodgson SF, Eastell R, Cedel SL, O'Fallon WM, Riggs BL. Cancellous bone remodeling in type I (postmenopausal) osteoporosis: quantitative assessment of rates of formation, resorption, and bone loss at tissue and cellular levels [see comments]. J Bone Miner Res 1990;5:311-9.
11. Eastell R. Treatment of postmenopausal osteoporosis. New Engl J Med 1998;338:736-46.
12. SBU (Swedish Council on Technology Assessment in Health Care). Bone density measurement—a systematic review: a report from SBU, the Swedish Council on Technology Assessment in Health Care. J Intern Med Suppl 1997;739:1-60.
13. Martin RB. Determinants of the mechanical properties of bones [published erratum appears in J Biomech 1992;25:1251]. J Biomech 1991;24 (suppl 1):79-88.

14. Goldstein SA, Goulet R, McCubbrey D. Measurement and significance of three-dimensional architecture to the mechanical integrity of trabecular bone. Calcif Tissue Int 1993;53 (suppl 1):S127-S132 (discussion S32-S33).
15. Goldstein SA. The mechanical properties of trabecular bone: dependence on anatomic location and function. J Biomech 1987;20:1055-61.
16. Gibson LJ. The mechanical behaviour of cancellous bone. J Biomech 1985;18:317-28.
17. Compston JE, Mellish RW, Garrahan NJ. Age-related changes in iliac crest trabecular microanatomic bone structure in man. Bone 1987;8:289-92.
18. Croucher PI, Garrahan NJ, Compston JE. Structural mechanisms of trabecular bone loss in primary osteoporosis: specific disease mechanism or early ageing? Bone Miner 1994;25:111-21.
19. Caligiuri P, Giger ML, Favus MJ, Jia He. Computerized radiographic analysis of osteoporosis: preliminary evaluation. Radiology 1993;186:471-4.
20. Croucher PI, Garrahan NJ, Compston JE. Assessment of cancellous bone structure: comparison of strut analysis, trabecular bone pattern factor, and marrow space star volume. J Bone Miner Res 1996;11:955-61.
21. Ito M, Ohki M, Hayashi K, Yamada M, Uetani M, Nakamura T. Trabecular texture analysis of CT images in the relationship with spinal fracture. Radiology 1995;194:55-9.
22. Majumdar S, Genant HK, Grampp S, Newitt DC. Correlation of trabecular bone structure with age, bone mineral density, and osteoporotic status: in vivo studies in the distal radius using high resolution magnetic resonance imaging. J Bone Miner Res 1997;12:111-8.
23. Haidekker MA, Andresen R, Evertsz CJ, Banzer D, Peitgen HO. Assessing the degree of osteoporosis in the axial skeleton using the dependence of the fractal dimension on the grey level threshold. Br J Radiol 1997;70:586-93.
24. Law AN, Bollen AM, Chen SK. Detecting osteoporosis using dental radiographs: a comparison of four methods. J Am Dent Assoc 1996;127:1734-42.
25. Southard TE, Southard KA, Jakobsen JR, Hillis SL, Najim CA. Fractal dimension in radiographic analysis of alveolar process bone. Oral Surg Oral Med Oral Pathol Oral Radiol Endod 1996;82:569-76.
26. Ruttimann UE, Webber RL, Hazelrig JB. Fractal dimension from radiographs of peridental alveolar bone: a possible diagnostic indicator of osteoporosis. Oral Surg Oral Med Oral Pathol 1992;74:98-110.
27. Geraets WG, Van der Stelt PF, Netelenbos CJ, Elders PJ. A new method for automatic recognition of the radiographic trabecular pattern. J Bone Miner Res 1990;5:227-33.
28. Geraets WG, van der Stelt PF. Analysis of the radiographic trabecular pattern. Pattern Recognition Letters 1991;12:575-81.
29. Geraets WG, Van der Stelt PF, Elders PJ. The radiographic trabecular bone pattern during menopause. Bone 1993;14:859-64.
30. Rasband W. NIH Image 1.61. http://rsb.info.nih.gov/nih-image/ 1997.
31. Horner K, Devlin H, Alsop CW, Hodgkinson IM, Adams JE. Mandibular bone mineral density as a predictor of skeletal osteoporosis. Br J Radiol 1996;69:1019-25.
32. Klemetti E, Vainio P, Lassila V, Alhava E. Cortical bone mineral density in the mandible and osteoporosis status in postmenopausal women. Scand J Dent Res 1993;101:219-23.
33. Horner K, Devlin H. Clinical bone densitometric study of mandibular atrophy using dental panoramic tomography. J Dent 1992;20:33-7.
34. Kribbs PJ. Comparison of mandibular bone in normal and osteoporotic women. J Prosthet Dent 1990;63:218-22.
35. Kribbs PJ, Chesnut CH, Ott SM, Kilcoyne RF. Relationships between mandibular and skeletal bone in an osteoporotic population. J Prosthet Dent 1989;62:703-7.
36. von Wowern N, Kollerup G. Symptomatic osteoporosis: a risk factor for residual ridge reduction of the jaws. J Prosthet Dent 1992;67:656-60.
37. Horner K, Devlin H. The relationships between two indices of mandibular bone quality and bone mineral density measured by dual energy X-ray absorptiometry. Dentomaxillofac Radiol 1998;27:17-21.
38. Taguchi A, Tanimoto K, Suei Y, Otani K, Wada T. Oral signs as indicators of possible osteoporosis in elderly women. Oral Surg Oral Med Oral Pathol Oral Radiol Endod 1995;80:612-6.
39. Taguchi A, Tanimoto K, Suei Y, Ohama K, Wada T. Relationship between the mandibular and lumbar vertebral bone mineral density at different postmenopausal stages. Dentomaxillofac Radiol 1996;25:130-5.
40. Hildebolt CF. Osteoporosis and oral bone loss. Dentomaxillofac Radiol 1997;26:3-15.
41. Taguchi A, Suei Y, Ohtsuka M, Otani K, Tanimoto K, Ohtaki M. Usefulness of panoramic radiography in the diagnosis of postmenopausal osteoporosis in women: width and morphology of inferior cortex of the mandible. Dentomaxillofac Radiol 1996;25:263-7.
42. Southard TE, Southard KA. Detection of simulated osteoporosis in maxillae using radiographic texture analysis. IEEE Trans Biomed Eng 1996;43:123-32.
43. Mellish RW, Garrahan NJ, Compston JE. Age-related changes in trabecular width and spacing in human iliac crest biopsies. Bone Miner 1989;6:331-8.
44. Garrahan NJ, Mellish RW, Compston JE. A new method for the two-dimensional analysis of bone structure in human iliac crest biopsies. J Microsc 1986;142:341-9.
45. Parfitt AM, Mathews CH, Villanueva AR, Kleerekoper M, Frame B, Rao DS. Relationships between surface, volume, and thickness of iliac trabecular bone in aging and in osteoporosis: implications for the microanatomic and cellular mechanisms of bone loss. J Clin Invest 1983;72:1396-409.
46. Geraets WG, Van der Stelt PF, Lips P, Van Ginkel FC. The radiographic trabecular pattern of hips in patients with hip fractures and in elderly control subjects. Bone 1998;22:165-73.
47. Vogel M, Hahn M, Delling G. Relation between 2- and 3-dimensional architecture of trabecular bone in the human spine. Bone 1993;14:199-203.
48. Mellish RW, Ferguson-Pell MW, Cochran GV, Lindsay R, Dempster DW. A new manual method for assessing two-dimensional cancellous bone structure: comparison between iliac crest and lumbar vertebra. J Bone Miner Res 1991;6:689-96.
49. Mundinger A, Wiesmeier B, Dinkel E, Helwig A, Beck A, Schulte-Moenting J. Quantitative image analysis of vertebral body architecture: improved diagnosis in osteoporosis based on high-resolution computed tomography. Br J Radiol 1993;66:209-13.
50. Korstjens CM, Mosekilde L, Spruijt RJ, Geraets WG, van der Stelt PF. Relations between radiographic trabecular pattern and biomechanical characteristics of human vertebrae. Acta Radiol 1996;37:618-24.
51. White SC, Rudolph DJ, Ma L. Influence of x-ray beam angulation and exposure on morphologic features of trabecular bone. Int J Oral Biol 1999;24:17-23.
52. Southard KA, Southard TE. Comparison of digitized radiographic alveolar features between 20- and 70-year-old women: a preliminary study. Oral Surg Oral Med Oral Pathol 1992;74:111-7.
53. Lang P, Steiger P, Faulkner K, Gluer C, Genant HK. Osteoporosis: current techniques and recent developments in quantitative bone densitometry. Radiol Clin North Am 1991;29:49-76.
54. Bender IB, Seltzer S. Roentgenographic and direct observation of experimental lesions in bone, I. J Am Dent Assoc 1961;62:27-34.
55. Russ JC. The image processing handbook. 2nd ed. Boca Raton: CRC Press; 1995.

Reprint requests:

Stuart C. White, DDS, PhD
UCLA School of Dentistry
53-068 Center for the Health Sciences
10833 Le Conte Avenue
Los Angeles, CA 90095-1668
swhite@dent.ucla.edu